

# Estimation of Gaussian Bi-Clusters with General Block-Diagonal Covariance Matrix and Applications

Anastasiia Livochka <sup>\*</sup>    Ryan Browne <sup>†</sup>    Sanjeena Subedi<sup>‡</sup>

February 9, 2023

## Abstract

Bi-clustering is a technique that allows for the simultaneous clustering of observations and features in a dataset. This technique is often used in bioinformatics, text mining, and time series analysis. An important advantage of biclustering algorithm is the ability to uncover multiple “views” (i.e., through rows and column groupings) in the data. Several Gaussian mixture model based biclustering approach currently exist in the literature. However, they impose severe restrictions on the structure of the covariance matrix. Here, we

---

<sup>\*</sup>Department of Statistics and Actuarial Science, 200 University Ave W, Waterloo, ON, N2L 3G1, Canada

<sup>†</sup>Department of Statistics and Actuarial Science, 200 University Ave W, Waterloo, ON, N2L 3G1, Canada. e: ryan.browne@uwaterloo.ca

<sup>‡</sup>School of Mathematics and Statistics, 4302 Herzberg Laboratories, Carleton University, 1125 Colonel By Drive, Ottawa, ON, K1S 5B6, Canada e: sanjeena.dang@carleton.ca

propose a Gaussian mixture model-based bi-clustering approach that provides a more flexible block-diagonal covariance structure. We show that the clustering accuracy of the proposed model is comparable to other known techniques but our approach provides a more flexible covariance structure and has substantially lower computational time. We demonstrate the application of the proposed model in bioinformatics and topic modelling.

**Keywords:** Bi-clustering, Gaussian mixture models

## 1 Introduction

Humans are particularly good at classifying objects into natural groups based on some notion of similarity and the goal they want to achieve. However, as the set of objects to organize and the number of features grows, we require faster and more memory-efficient tools to complete the task. Cluster analysis is an important area of unsupervised machine learning that deals with the problem of grouping objects so that objects in one cluster are more similar to each other than to objects in other clusters (Diday and Simon, 1976). The main applications of cluster analysis include data exploration and pattern recognition (Berkhin, 2006).

Cluster analysis has been widely studied for decades, and many clustering algorithms have been developed. Interestingly, the great variety of the available models can be attributed to the fact that precisely defining a cluster presents a problem (Milligan and Cooper, 1987). Some algorithms (e.g. DBSCAN, HDBSCAN) leverage density assumptions by defining clusters as connected dense regions in the space (Khan et al., 2014; McInnes et al., 2017). Other approaches view clusters as mix-

tures of certain distributions, with Gaussian mixture model (GMM) being the most popular one (Reynolds, 2009).

Bi-clustering is a technique that allows for the simultaneous clustering of observations and features in a dataset (Hartigan, 1972). An important advantage of bi-clustering is the ability to uncover multiple “views” (i.e., through row and column groupings) in the data. This technique is often used in bioinformatics, text mining, and time series analysis (Madeira and Oliveira, 2004; Madeira et al., 2008; Busygin et al., 2008). For example, Wang et al. (2013) utilized biclustering algorithm on gene expression data and identified subgroups of breast cancer tumour with similar clinical characteristics. In topics modelling context, it’s been extensively used to interpret the resulting clusters (Rugeles et al., 2017).

There is no single definition of a cluster and as such there is no single definition of a bi-cluster. Therefore, a variety of bi-clustering models exist. One of the first applications of bi-clustering to text documents is based on the spectral graph (Dhillon, 2001) partitioning heuristic. Similarly, Kluger et al. (2003) shows that the checker-board structure of the data matrix can be inferred from its eigenvectors. There are many greedy approaches proposed for the co-clustering of gene expressions (Padilha and Campello, 2017; Cheng and Church, 2000; Bergmann et al., 2003). For instance, Ben-Dor et al. (2002) introduces an approach that finds the hidden order-preserving sub-matrices in the data matrix.

Alternate model-based biclustering approaches assume that the observations in the same row cluster were generated from the same distribution. e.g.  $\mathcal{N}_p(\boldsymbol{\mu}, \boldsymbol{\Sigma})$ . In turn, column groups can be inferred from the structure of the covariance matrix.

Suppose we have a  $p$ -dimensional mean vector  $\boldsymbol{\mu}$  such that

$$\boldsymbol{\mu} = [\boldsymbol{\mu}_1, \boldsymbol{\mu}_2, \boldsymbol{\mu}_3],$$

where the dimensions of  $\boldsymbol{\mu}_i$  is  $c_i$ ,  $i = 1, \dots, 3$  and  $p = c_1 + c_2 + c_3$ , and covariance matrix,  $\boldsymbol{\Sigma}$ , can be written as:

$$\boldsymbol{\Sigma} = \text{diag}(\boldsymbol{\Sigma}_1, \boldsymbol{\Sigma}_2, \boldsymbol{\Sigma}_3) = \begin{bmatrix} \boldsymbol{\Sigma}_{1(c_1 \times c_1)} & \mathbf{0} & \mathbf{0} \\ \mathbf{0} & \boldsymbol{\Sigma}_{2(c_2 \times c_2)} & \mathbf{0} \\ \mathbf{0} & \mathbf{0} & \boldsymbol{\Sigma}_{3(c_3 \times c_3)} \end{bmatrix}. \quad (1)$$

Then  $(\boldsymbol{\mu}_1, \boldsymbol{\Sigma}_1), (\boldsymbol{\mu}_2, \boldsymbol{\Sigma}_2), (\boldsymbol{\mu}_3, \boldsymbol{\Sigma}_3)$  define three distinct column groupings. Note that column permutations may be required to achieve a checkerboard-like structure as illustrated in 1. This adds to the non-triviality of the estimation of block-diagonal covariance matrix.

Initial model-based bi-clustering approaches introduced additional latent variables to indicate column clusters (Bhatia et al., 2014; Gu and Liu, 2008). Gallagher et al. (2022) proposed a Gaussian model-based clustering for high-dimensional data. They partition columns of the dataset twice - once by means and another by variances. Others (Martella et al., 2008; Wong et al., 2017; Tu and Subedi, 2022) leveraged the bi-clustering framework rooted in the mixtures of factor analyzers (McNicholas and Murphy, 2008) approach. The advantage of the factor analyzer structure is that it decreases the number of estimated parameters by assuming a latent low-dimensional representation of high-dimensional variables. However, this

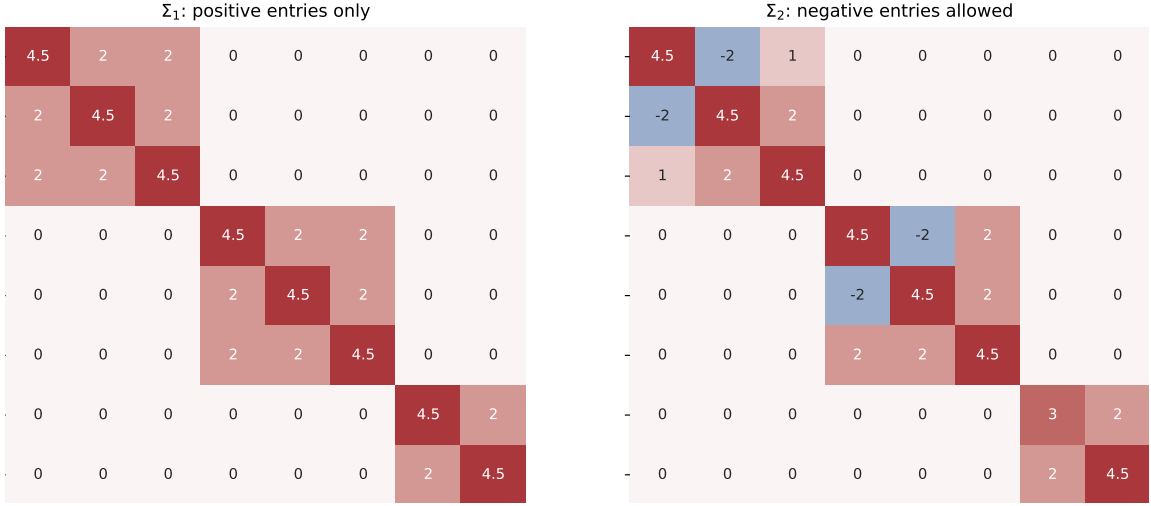


Figure 1: Illustration of the block diagonal matrices with off-diagonal elements limited to positive (*left*) and general (*right*) structure.

representation restricts the covariance matrix structure that can be recovered. For example, Martella et al. (2008) and Wong et al. (2017) require the within block off-diagonal elements of the covariance matrix to be 1. Tu and Subedi (2022) relaxed some constraints by characterizing covariance to allow the all of the off-diagonal entries of  $i$ -th covariance block to be equal to a positive constant. This is illustrated in the left panel of Figure 1. In addition, the parameter estimation utilized in Martella et al. (2008); Wong et al. (2017); Tu and Subedi (2022) has limitations due to the complexity of finding column groupings.

In this work, we aim to build on the model-based bi-clustering procedure by allowing the covariance matrix of the underlying mixture components to have a general block-diagonal structure as shown in the right panel of Figure 1. We derive and compare three approaches to estimate the column groupings; greedy, convex relaxation and hierarchical. Empirically the hierarchical approach is shown to be the

best approach in terms of accuracy and computational efficiency. We also compare the hierarchical approach to readily available covariance matrix estimators (Ledoit and Wolf, 2004; Friedman et al., 2008; Broto et al., 2022). The readily available approaches do not satisfy our desirable conditions for the covariance estimator, namely (i) enforcing the block-diagonal structure on the covariance matrix; and (ii) allowing for general covariance matrix structure inside the blocks. In the second half the manuscript, we introduce the model-based bi-clustering procedure with the general block-diagonal structure. We use simulated datasets to determine the efficacy of the model. We show utility of our approach in bioinformatics and topics modelling. First, we applied the proposed model and other existing bi-clustering models on two high-dimensional genomics classification problems: **Alon** (Alon et al., 1999) and **Golub** (Golub et al., 1999) datasets. Then, we illustrate the proposed methodology on two datasets from topic modelling: hotel ratings & reviews (Alam et al., 2016) and Disneyland ratings & reviews (Chillar, 2022).

## 2 Estimating a Block-Diagonal Covariance Matrix

This section discusses parameterization of a block-diagonal matrix and its estimation. We propose three methods for estimating the block-diagonal covariance matrix (as illustrated on the 1 - which is crucial for the GMM-based bi-clustering procedure given section 3. For simplicity, we derive an estimation for one component of GMM here. In Section 3, we extend the techniques for multi-component mixture model. The main aim of this work is to propose an approach such that: (i) it imposes

a block-diagonal structure onto the covariance matrix; (ii) it does not restrict the covariance matrix structure inside the blocks.

## 2.1 Imposing Block-Diagonal Structure Onto a Covariance Matrix

Suppose we have a normally distributed data  $\mathbf{X} \sim \mathcal{N}_p(\boldsymbol{\mu}, \boldsymbol{\Sigma})$ . One way to compute feature clusters, common for biclustering, is by estimating a block-diagonal covariance matrix that is close to the original  $\boldsymbol{\Sigma}$ . In this work, we propose to parameterize this block-diagonal covariance matrix as:

$$\mathbf{D}_1^T \boldsymbol{\Sigma} \mathbf{D}_1 + \cdots + \mathbf{D}_K^T \boldsymbol{\Sigma} \mathbf{D}_K \quad \text{where} \quad \mathbf{D}_1 + \cdots + \mathbf{D}_K = \mathbf{I}_p \quad (2)$$

where,  $K$  is the number of variable or column groups,  $\mathbf{D}_k = \text{diag}(\mathbf{d}_k)$  and each element of  $\mathbf{d}_k$  is zero or one. In other words, the  $\mathbf{D}_k$  are binary diagonal matrices that sum up to the identity matrix. This allows for each  $\mathbf{D}_k$  to define a column or feature group  $k$  using  $\mathbf{D} = [\mathbf{d}_1, \dots, \mathbf{d}_K]$ . For example, to get the general covariance structure in Figure 1, we set

$$\mathbf{D} = \begin{bmatrix} \mathbf{d}_1 & \mathbf{d}_2 & \mathbf{d}_3 \end{bmatrix} = \begin{bmatrix} 1 & 1 & 1 & 0 & 0 & 0 & 0 & 0 \\ 0 & 0 & 0 & 1 & 1 & 1 & 0 & 0 \\ 0 & 0 & 0 & 0 & 0 & 0 & 1 & 1 \end{bmatrix}^T. \quad (3)$$

This proposed parametrization imposes a general block-diagonal structure on the covariance matrix. i.e. we can obtain the general covariance structure shown in the

right panel of Figure 1.

If we have a sample  $\{\mathbf{x}_1, \mathbf{x}_2, \dots, \mathbf{x}_N\}$  generated from a  $p$ -dimensional multivariate Gaussian with mean,  $\boldsymbol{\mu}$ , and a positive definite covariance matrix,  $\boldsymbol{\Sigma}$ . The scaled or normalized log-likelihood is

$$-\frac{1}{2} \log |\boldsymbol{\Sigma}| - \frac{1}{2N} \sum_{i=1}^N \text{tr} [\boldsymbol{\Sigma}^{-1}(\mathbf{x}_i - \hat{\boldsymbol{\mu}})(\mathbf{x}_i - \hat{\boldsymbol{\mu}})^\top].$$

The maximum likelihood estimates (MLEs) of the parameters  $\boldsymbol{\mu}$  and  $\boldsymbol{\Sigma}$  are the sample mean and sample covariance:

$$\hat{\boldsymbol{\mu}} = \bar{\mathbf{x}} = \frac{\sum_{i=1}^N \mathbf{x}_i}{N}, \quad \text{and} \quad \mathbf{S} = \frac{\sum_{i=1}^N (\mathbf{x}_i - \hat{\boldsymbol{\mu}})(\mathbf{x}_i - \hat{\boldsymbol{\mu}})^\top}{N}.$$

Furthermore, we denote sample correlation matrix by  $\mathbf{S}^*$ .

Since, the MLE for unconstrained covariance matrix is  $\mathbf{S}$ , the log-likelihood function for the block diagonal covariance matrix as a function of the feature groups,  $\mathbf{D} = [\mathbf{d}_1, \dots, \mathbf{d}_K]$ , is

$$\mathcal{L}(\mathbf{d}_1, \dots, \mathbf{d}_K) = -\frac{1}{2} \log \left| \sum_{k=1}^K \mathbf{D}_k \mathbf{S} \mathbf{D}_k \right| - \frac{1}{2} \text{tr} \left[ \left( \sum_{k=1}^K \mathbf{D}_k \mathbf{S} \mathbf{D}_k \right)^{-1} \mathbf{S} \right] \quad (4)$$

where  $\mathbf{D}_k = \text{diag}(\mathbf{d}_k)$ . In the next three sections, we discuss three approaches to estimate  $\mathbf{D}$ : greedy, convex relaxation (numerical) and hierarchical.



## 2.2 Greedy Approach

Motivated by the approach in Tu and Subedi (2022), we decided to adopt a greedy algorithm for estimating  $\mathbf{D} = [\mathbf{d}_1, \dots, \mathbf{d}_K]$  in (4). To initialize we follow Tu and Subedi (2022) and set  $\mathbf{D}$  to the first  $K$  principal components of the correlation matrix  $\mathbf{S}^*$ . Then, in the  $j^{th}$  row of  $\mathbf{D}$ , we find the largest element, e.g. the  $k^{th}$  element, set that element to one and then the remaining are set zero. This can be interpreted as assigning the  $j$ -th row to the  $k^{th}$ -the column group.

After initialization, we iteratively reassign column clusters similar to the initialization but instead we use the largest log-likelihood value (4). Starting with variable  $j$ , we evaluate the equation (4) by considering this feature or variable in each of the  $K$  feature group and assign the variable to the  $k^{th}$  column group that maximizes the log-likelihood. Alternatively, this is equivalent to considering each of the unit vectors, of length  $K$  in the row  $j^{th}$  of  $\mathbf{D}$ . Mathematically, for the  $j^{th}$  row of  $\mathbf{D}$ , denoted by  $\mathbf{D}_j$ , we have

$$\mathbf{D}_j = \arg \max_{\mathbf{a} \in \{\mathbf{e}_1, \dots, \mathbf{e}_K\}} \mathcal{L}(\mathbf{d}_1, \dots, \mathbf{d}_{j-1}, \mathbf{a}, \mathbf{d}_{j+1}, \dots, \mathbf{d}_K)$$

for  $j = 1, \dots, p$  and  $\mathbf{e}_k$  is a unit vector of length  $K$  which has a unit in the  $k^{th}$  position and zero elsewhere. This means each updated row is conditional on the rest of them.

### 2.3 Convex Relaxation Approach

We aim to find  $\mathbf{D} = [\mathbf{d}_1, \mathbf{d}_2, \dots, \mathbf{d}_K]$  that maximizes log-likelihood in (4). Keeping in mind that  $\mathbf{d}_k$  should be binary by definition of (2), this is a non-linear integer problem, which is known for its complexity (Hemmecke et al., 2009). To simplify, we relaxed the  $\mathbf{d}$  binary constraints and use quadratic programming to solve the following:

$$\max \mathcal{L} \quad \text{st.} \quad \forall k : \mathbf{d}_k > \mathbf{0} \quad \text{and} \quad \sum_{k=1}^K \mathbf{d}_k = \mathbf{1} \quad (5)$$

where  $\mathbf{d}_k > \mathbf{0}$  means that each element of  $\mathbf{d}_k$  should be greater than zero. This relaxes the condition that the  $\mathbf{D}_k$  are binary diagonal matrices by allow each element of  $\mathbf{D}_k$  to be positive. A possible solution is that  $\forall k : \mathbf{d}_k = 1/K \times \mathbf{1}$  as it results in  $\mathbf{\Sigma} = \mathbf{S}$ . To avoid the trivial solution, we added a penalty on the logarithm of the determinant of  $\mathbf{D}^\top \mathbf{D}$ . Then in addition we will use a penalty to push  $\mathbf{d}_k$  towards binary values. In particular the penalty is  $\sum_{k=1}^K \mathbf{d}_k^\top \mathbf{d}_k - p$ . Finally, instead of applying a block diagonal structure to the covariance, we apply it to the inverse of the covariance matrix also known as the precision matrix. Note that the two parameterizations are equivalent because the inverse of a block diagonal matrix is block diagonal matrix. However, using the precision matrix will simplify the derivatives.

The parameterized block diagonal precision matrix is

$$\mathbf{D}_1 \mathbf{\Sigma}^{-1} \mathbf{D}_1 + \dots + \mathbf{D}_K \mathbf{\Sigma}^{-1} \mathbf{D}_K. \quad (6)$$

We want to maximize the log-likelihood function with respect to the block-diagonal structure of the covariance matrix: The MLE for  $\mathbf{\Sigma}^{-1}$  is  $\mathbf{S}^{-1}$  so putting (4) in terms

of the precision matrix we have

$$\mathcal{L}^*(\mathbf{d}_1, \dots, \mathbf{d}_K) \frac{1}{2} \log \left| \sum_{k=1}^K \mathbf{D}_k \mathbf{S}^{-1} \mathbf{D}_k \right| - \frac{1}{2} \text{tr} \left[ \left( \sum_{k=1}^K \mathbf{D}_k \mathbf{S}^{-1} \mathbf{D}_k \right) \mathbf{S} \right] \quad (7)$$

We utilize the properties of the trace and element-wise product operators to obtain

$$\text{tr}(\mathbf{D}_k \mathbf{S}^{-1} \mathbf{D}_k \mathbf{S}) = \mathbf{d}_k^T (\mathbf{S}^{-1} \odot \mathbf{S}) \mathbf{d}_k \quad (8)$$

where  $\odot$  is element-wise or Hadamard product.

Combing the penalties and the log-likelihood function we have

$$\mathcal{F}^*(\mathbf{d}_1, \dots, \mathbf{d}_K) = \mathcal{L}^*(\mathbf{d}_1, \dots, \mathbf{d}_K) + \gamma \left( \sum_{k=1}^K \mathbf{d}_k^T \mathbf{d}_k - m \right) - \lambda \log |\mathbf{D}^T \mathbf{D}| \quad (9)$$

for  $\gamma, \lambda \in \mathbb{R}^+$ . This optimization problem can be solved numerically utilizing gradient descent. Gradient descent is an iterative, first-order optimization method that finds local minima or maxima of the differentiable function. We propose to estimate the columns of  $\mathbf{D}$  iteratively conditioning on the values of all other column vectors.

To compute the partial derivatives of (9) with respect to  $\mathbf{d}_k$ , we note that  $\mathbf{D}_k = \text{diag}(\mathbf{d}_k)$  and  $\partial \text{diag}(\mathbf{d}_k) = \text{diag}(\partial \mathbf{d}_k)$ . The partial derivative is

$$\frac{\partial \mathcal{F}^*}{\partial \mathbf{d}_k} = [\mathbf{T} \odot \mathbf{S}^{-1}] \mathbf{d}_k - (\mathbf{R}^{-1} \odot \mathbf{R}) \mathbf{d}_k + 2\gamma \mathbf{d}_k - 2\lambda [\mathbf{D}(\mathbf{D}^T \mathbf{D})^{-1}]_k \quad (10)$$

where  $\mathbf{T} = (\sum_{k=1}^K \mathbf{D}_k \mathbf{S}^{-1} \mathbf{D}_k)^{-1}$  and  $[\mathbf{A}]_k$  denotes the  $k$ -th column of the matrix  $\mathbf{A}$ . To maximize the  $\mathcal{F}^*$ , we take a step in the direction of a positive gradient. Let us

denote  $\omega \in \mathbb{R}$  to be a learning rate, then the proposed update for  $\mathbf{d}_k$  is defined as:

$$\mathbf{d}_k^{(t+1)} = \mathbf{d}_k^{(t)} + \omega \frac{\partial \mathcal{F}^*}{\partial \mathbf{d}_k}. \quad (11)$$

Through some experimentation, setting  $\omega = 0.1$  worked well in all the simulations.

## 2.4 Hierarchical Clustering Approach

Hierarchical clustering refers to a widely utilized family of clustering algorithms (Murtagh and Legendre, 2014; Beeferman and Berger, 2000; Erica et al., 2018), that are based on an iterative procedure of either merging or splitting nested clusters. Merging or splitting is also known as bottom-up and top-down approaches correspondingly. Many readily available implementations and generalizations of the algorithm ensure robustness on various input data configurations (Balcan et al., 2014).

Here, we leverage the bottom-up hierarchical approach known as agglomerative clustering to find the column clusters. However, instead of clustering the transpose of the dataset, we propose to use the absolute values of correlations as a feature representations for each variable. The absolute value will remove the effect of positive and negative correlations. Then we apply agglomerative clustering to the feature representations. To obtain the variables features, if  $\mathbf{S}^*$  is the estimate of the correlation matrix based on dataset and  $\mathbf{S}$  is the MLE of the covariance matrix, we calculate

$$\mathbf{R}^* = |\mathbf{S}^*| = \left| \text{diag}(\mathbf{S})^{-\frac{1}{2}} \mathbf{S} \text{diag}(\mathbf{S})^{-\frac{1}{2}} \right| \quad (12)$$

where  $|\mathbf{A}|$  applies the absolute value element-wise to the matrix  $\mathbf{A}$  and  $\text{diag}(\mathbf{A})$

creates a diagonal matrix using the diagonal elements of the matrix  $\mathbf{A}$ . Treating  $\mathbf{R}^*$  as feature vectors, we then use the  $l_2$ -norm to construct a distance matrix. This distance results in variables with similar correlation vectors to be close to each other.

The agglomerative clustering procedure starts by assigning every variable into its own group. On every iteration, it merges two of the most similar groups, as measured by a selected similarity/dissimilarity metric, which is known as linkage criteria. The linkage criterion is a metric that defines the distance between two clusters. There are three most widely used linkage criteria (Vijaya et al., 2019): single linkage, complete linkage and average linkage. single, complete and average linkage defines distance between two clusters as the minimum, maximum or average distance among distances between the two clusters, respectively. We propose utilizing average linkage criteria as this method results in clusters with the highest cohesion as discussed in Sokal and Michener (1958). Once the  $K$  variable groups have been obtained, we construct the corresponding block diagonal covariance matrix.

## 2.5 Comparison & Experiments

In this subsection, we aim to conduct experiments with simulated data to establish which of the three proposed approaches for estimating the block-diagonal matrix is the most accurate and efficient. Section 2.5.1 compares the execution time and accuracy of the three approaches while varying the number of observations in the dataset. We find that the hierarchical approach is the the most accurate and efficient one.

The we compare the hierarchical approach to other known covariance estimators.

In the 2.5.2 we experiment with recovering two different structures of the covariance matrix with our vs state-of-the-art approaches, including the shrinkage estimator (Ledoit and Wolf, 2004), Graphical Lasso (Friedman et al., 2008), factor-analyzer UCUU (Tu and Subedi, 2022) and MLE. We find that methods that artificially enforce block-diagonal covariance structure are more accurate and the proposed method is indeed more robust than the UCUU model (Tu and Subedi, 2022) for matrices with negative covariances.

Finally, we investigate the limitations of the hierarchical estimator by increasing the complexity the block-diagonal matrix  $\Sigma$  when the number of columns group is known and unknown. We examine using the maximum silhouette score (Rousseeuw, 1987) to determine the number of groups. We discovered that the usage of the hierarchical algorithm is limited when estimating high number of small blocks.

### 2.5.1 Accuracy and Efficiency of the three Proposed Estimation Approaches

In this subsection, we investigate the accuracy and efficiency of the three proposed approaches to the problem of recovering column clusters  $\mathbf{D}_k$ . The experiment setup is similar to other proposed in Tu and Subedi (2022). In this subsection, we generate  $N$  observations from  $p = 8$  dimensional Gaussian distribution with  $\boldsymbol{\mu} = (0, 1, 2, 3, 4, 5, 6, 7)^\top$  and two different covariance matrices. Figure 1 displays two options for the covariance matrix that are considered in the experiments:  $\Sigma_A$  with only non-negative off-diagonal entries;  $\Sigma_B$  with negative off-diagonal entries.  $\Sigma_A$  and  $\Sigma_B$  are both block diagonal matrices displayed in Figure 1. For case A, we

have  $\Sigma_A = \text{diag}(\Sigma_{A1}, \Sigma_{A2}, \Sigma_{A3})$  where

$$\Sigma_{A1} = \begin{bmatrix} 4.5 & 2 & 2 \\ 2 & 4.5 & 2 \\ 2 & 2 & 4.5 \end{bmatrix}, \quad \Sigma_{A2} = \begin{bmatrix} 4.5 & 2 & 2 \\ 2 & 4.5 & 2 \\ 2 & 2 & 4.5 \end{bmatrix}, \quad \Sigma_{A3} = \begin{bmatrix} 4.5 & 2 \\ 2 & 4.5 \end{bmatrix},$$

and for case B, we have  $\Sigma_B = \text{diag}(\Sigma_{B1}, \Sigma_{B2}, \Sigma_{B3})$  where

$$\Sigma_{B1} = \begin{bmatrix} 4.5 & -2 & 1 \\ -2 & 4.5 & 2 \\ 1 & 2 & 4.5 \end{bmatrix}, \quad \Sigma_{B2} = \begin{bmatrix} 4.5 & -2 & 2 \\ -2 & 4.5 & 2 \\ 2 & 2 & 4.5 \end{bmatrix}, \quad \Sigma_{B3} = \begin{bmatrix} 3 & 2 \\ 2 & 4.5 \end{bmatrix}.$$

The choice of covariance matrices is motivated by restrictions for off-diagonal elements to be strictly non-negative utilized commonly in the literature (Wong et al., 2017; Tu and Subedi, 2022; Martella et al., 2008). To goal here is to recover a covariance matrix of the general structure, including the possibility of negative off-diagonal elements. Note that both matrices in Figure 1 have a natural block-diagonal structure, which provides us with ground truth for column cluster indicator matrices  $\mathbf{D}_k$  as shown previously in (3).

Figure 2 shows results with data generated from  $\mathcal{N}(\boldsymbol{\mu}, \Sigma_A)$ . We vary the number of data points,  $N = 50, 80, 100, 200, 500, 800, 1600$ , to understand the impact on both accuracy and execution time of the proposed methods. For every size  $N$ , we run the experiment 200 times and set number of column clusters to three. The accuracy is calculated as the total number of times when an algorithm returned correct column groups  $\mathbf{D}$  divided by the total number of attempts. 2 (*right*) demonstrates the

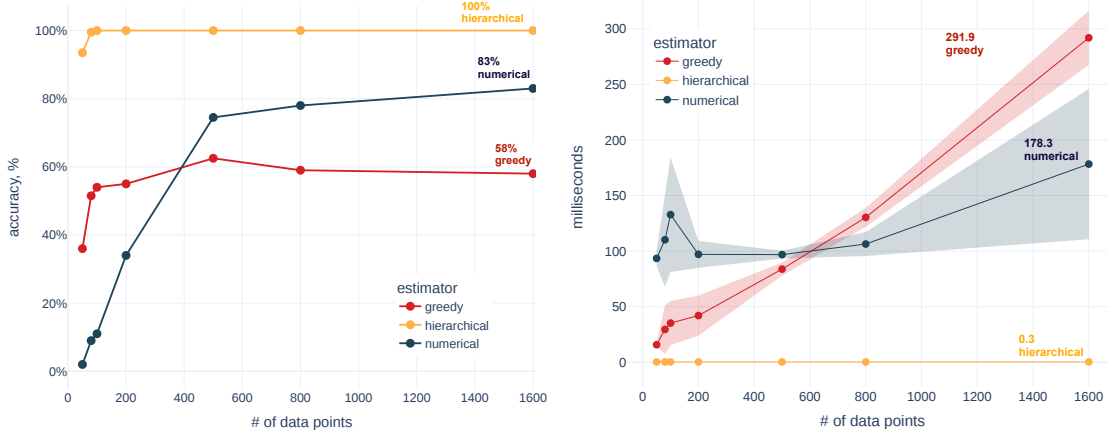


Figure 2: Comparison of accuracy & execution time over 200 runs for estimating  $D_k$  for block-diagonal  $8 \times 8$  covariance matrix with 3 blocks defined by  $\Sigma_A$  which has only positive entries. (*Left*) The accuracy of the proposed approaches is given a number of the data points in the generated dataset  $X$ . (*Right*) Execution time of the proposed approaches.

average execution time in milliseconds over 200 runs together with its standard deviation.

From Figure 2, it is clear that the hierarchical estimator for the column groups  $D_k$  is both accurate and efficient. It gets to 100% starting from 100 data points in the training set and demonstrates solid accuracy  $> 90\%$  even with  $N = 50$ . The numerical estimator benefits from the increasing dataset size. However, the time it needs to converge grows as well. In this experiment, the greedy estimator proved to be the least efficient and the least accurate for larger sample sizes.

Figure 3 demonstrates the results of the analogous experiment with data generated from  $\mathcal{N}(\mu, \Sigma_B)$ . Interestingly, the execution time of both numerical and greedy estimators increases. While the numerical estimator demonstrates degraded accuracy, the greedy one improves in the presence of negative covariances or a greater



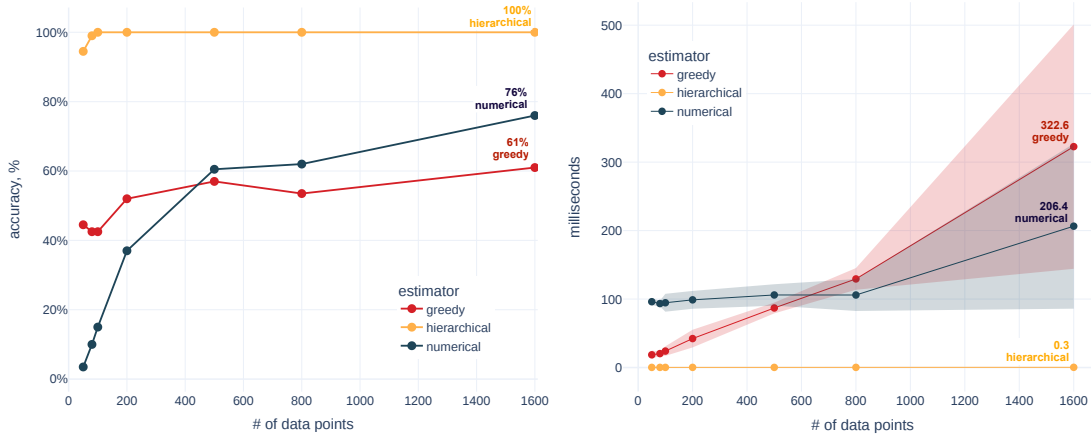


Figure 3: Comparison of accuracy & execution time for estimating  $D_k$  for block-diagonal  $8 \times 8$  covariance matrix with 3 blocks defined by  $\Sigma_B$  which has some negative entries. (*Left*) The accuracy of the proposed approaches given a number of the data points in the generated dataset  $X$ . (*Right*) Execution time of the proposed approaches.

variety of values within a covariance block. At the same time, the hierarchical approach leads in terms of both efficiency and accuracy, and it can correctly cluster columns even for the matrix with negative covariances. Therefore, for the following experiments, we proceed with the hierarchical approach.

### 2.5.2 Recovering Block-Diagonal Covariance Matrix & Comparison with the Literature

In this section, we evaluate the accuracy of estimation of the block-diagonal covariance matrix  $\Sigma$  using the mean absolute percentage error (MAPE). For estimating  $\Sigma$  with an estimate  $\hat{\Sigma}$ , we compute MAPE % measure as following:

$$100 \times \frac{\sum_{i,j} |\sigma_{ij} - \hat{\sigma}_{ij}|}{\sum_{i,j} \sigma_{ij}}. \quad (13)$$

We compare the hierarchical approach to the MLE and three other methods utilized in the literature: shrinkage estimator (Ledoit and Wolf, 2004), Graphical Lasso (Friedman et al., 2008) and UCUU model (Tu and Subedi, 2022).

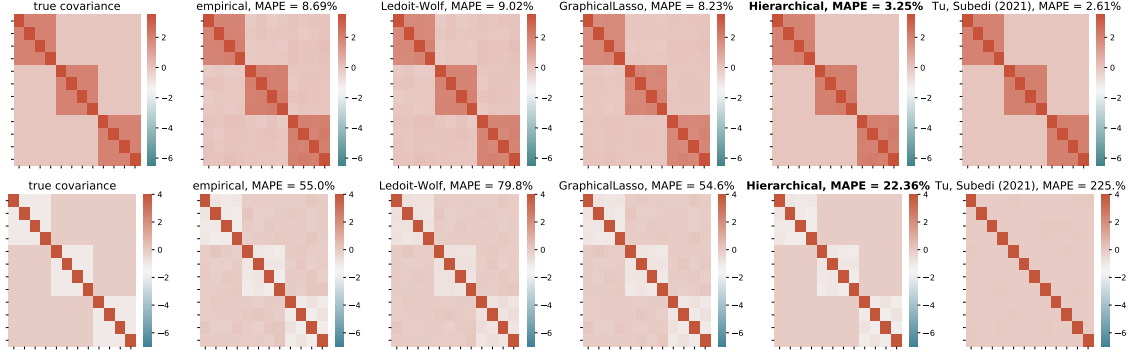


Figure 4: Average estimations over ten runs of recovering block-diagonal covariance matrix with only positive (*top*) / negative (*bottom*) off-diagonal entries with five methods including MLE (empirical), Ledoit-Wolf, Graphical Lasso, Hierarchical (proposed) & UCUU model by Tu and Subedi (2021). For standard deviations, see A.

The first column of Figure 4 shows two block-diagonal covariance matrices used to generate data-sets. The top row has a block-diagonal covariance matrix with 4.5 on the diagonal and 2 on the off-diagonals within a block. The bottom row has a block-diagonal covariance matrix with 4.5 on the diagonal and  $-1$  on the off-diagonals within a block. We use  $N = 300$ ,  $p = 12$  and  $\boldsymbol{\mu} = (1, 2, \dots, 12)$ . Every estimation of the covariance matrix is replicated ten times with the average  $\hat{\Sigma}$  for each estimator depicted in Figure 4. For the hierarchical approach and UCUU model (Tu and Subedi, 2022) we set the number of column groups to three.

Our analysis show that artificially enforcing block-diagonal covariance structure is justified for the problems when such covariance structure is expected. Note that

hierarchical approach and UCUU model are at least two times more accurate (in terms of MAPE) than others when the off-diagonal elements in the blocks are positive. On the other hand, the proposed hierarchical method is robust in the presence negative off-diagonal covariances, while the performance of the UCUU model by Tu and Subedi (2022) suffers dramatically as it is not designed for such case.

Note that, MAPE is only helpful for relative algorithm accuracy comparison but not for absolute estimation quality assessment. It allows the comparisons of the form “method X is 2 times more accurate than Y”. However, we do not deduce that all methods are highly inaccurate for the covariance matrix with negative off-diagonal entries because the denominator of equation 13 is small. Therefore even small errors will result in large percentages.

## 2.6 Impact of the Covariance Block Structure on the Performance of Hierarchical Estimator

In this section, we investigate the limitations of the hierarchical estimator by increasing the complexity the block-diagonal matrix  $\Sigma$  when the number of columns group is known and unknown. We measure the accuracy of the estimated column groups compared the generated column groups. The complexity of the variable groups  $\mathbf{D}$  is influenced by the dimensionality of number of features variables (i.e. columns) in the dataset,  $p$ ; and the number of blocks or column groups,  $K$ . We fix the number of rows in the dataset to  $N = 50$  and vary  $p$  and  $K$  to understand its impact on the estimator’s accuracy. This choice is motivated by common real-life scenarios (e.g. genomics, natural language processing etc.) when the number of observations

is often limited compared to the number of potential features.

We evaluate the accuracy of the hierarchical estimator with three different levels for the number of variables,  $p$ , and the number of blocks or variable groups,  $K$ . They will be referenced as low, medium and high and summarized in Table 1. The number of column groups at every level is proportional to number of variables. For example, for the low-low setting  $(p, K) = (24, 3)$  while the medium-low setting has  $(p, K) = (96, 4)$ . For simplicity, the number of variables within each block is set to  $p/K$ .

$(p, K)$ # of column groups - $K$	# of variables - $p$		
	low	medium	high
low	(24, 3)	(96, 4)	(384, 8)
medium	(24, 6)	(96, 8)	(384, 16)
high	(24, 12)	(96, 16)	(384, 32)

Table 1: Summary of different combinations of the number of variables,  $p$ , and the number of variable groups,  $K$ , in  $\Sigma$ . We set  $K$  dynamically in relation to  $p$  (e.g. low number of blocks is 3 for the data with 24 variables and 12 for the high-dimensional data with 384 columns)

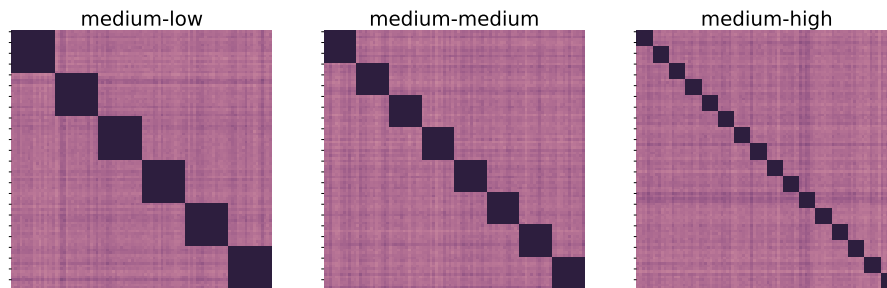


Figure 5: Examples of the covariance matrices  $\Sigma$  used to generate data for the simulation study. These show when the number of columns is set to medium  $p = 96$  and the number of blocks,  $k$  varies from 6 (low), 8 (medium) and 16 (high). Note the added noise.

For every combination of  $p$  and  $K$ , we run the analysis 500 times. In every run, we sample the elements of  $\boldsymbol{\mu}$  randomly from the uniform  $[0, 1]$  distribution. For the block diagonal covariance matrix, each block,  $\boldsymbol{\Sigma}_k$ , is set to  $\mathbf{A}^\top \mathbf{A}$  where  $\mathbf{A}$  is  $p/K$ -dimensional square matrix and the entries are generated from uniform  $U(1, 2)$ . Once each block has been constructed, we add random noise to the overall covariance matrix  $\boldsymbol{\Sigma}$  to bring this simulation closer to real-world scenarios. The random noise is equal to  $0.5\mathbf{E}^\top \mathbf{E}$  where  $\mathbf{E}$  is  $p$ -dimensional square matrix and the entries are generated from uniform  $U(0, 1)$ .

Figure 6 demonstrates the accuracy of the hierarchical estimator for different problem complexities in two scenarios: known vs an unknown actual number of column clusters (blocks of the covariance matrix). In the second case, we pick the number of groups that produces the maximum silhouette score (Rousseeuw, 1987) with the search range  $K \pm 2\sqrt{p}$ , where  $K$  is the number of clusters and  $p$  is a dimensionality of the data.

Figure 6 shows that the proposed estimator is accurate for the covariance structures in the low- and medium- setting data but has difficulty in the high-dimensional ( $p = 384$ ) setting. Although this might be due the sample size to be fixed at 50). We see that accuracies for the known vs unknown number of blocks are similar, which signifies the usefulness of the estimator even in the case when the number of column clusters is unknown.

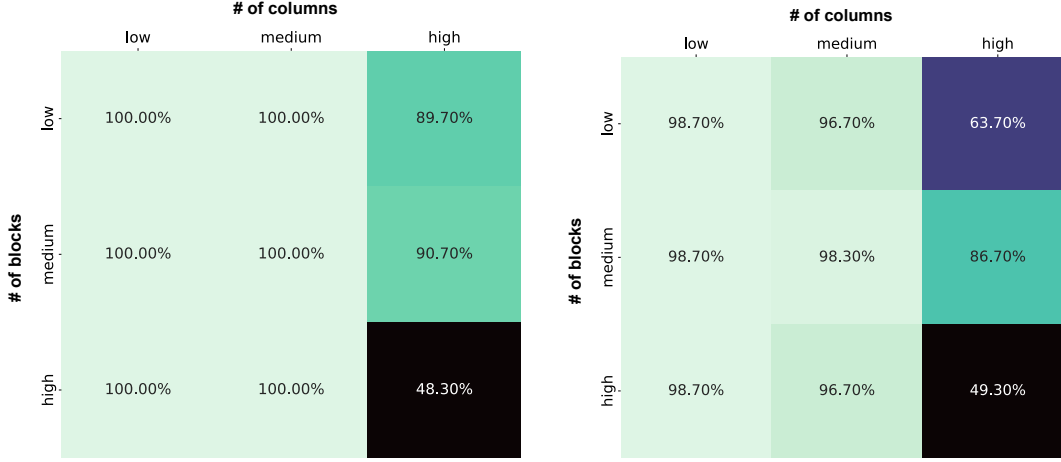


Figure 6: The average accuracy of the hierarchical estimator for the number of column groups  $\mathbf{D}$  while number of variables and the number column groups different complexities defined by the dimensionality of the dataset (low-high) and the true number of blocks in the covariance matrix  $\Sigma$  (number of column clusters). Tested for the scenario of known (*left*) and unknown (*right*)  $K$  clusters

### 3 The Bi-Clustering Model with general block diagonal structure

This section extends the proposed block diagonal structure and estimation procedure for model-based bi-clustering. We start by defining a probability density function for a finite  $G$ -component finite Gaussian mixture model (GMM),

$$g(\mathbf{x}_i | \boldsymbol{\theta}) = \sum_{g=1}^G \pi_g f(\mathbf{x}_i | \boldsymbol{\mu}_g, \Sigma_g) \quad (14)$$

where  $\pi_g > 0$ ,  $\sum_{g=1}^G \pi_g = 1$  and  $\boldsymbol{\theta}$  represents all the model parameters. For bi-clustering model, we assume that  $\Sigma_g$  has a block structure as given (2). The biggest difference between the proposed model and existing models based on the factor-

analyzer model is in how the covariance matrices are constructed.

There is no closed-form solution for estimating the parameters of the Gaussian mixture model. Parameters of such models are usually estimated by leveraging the expectation-maximization (EM; Dempster et al., 1977) algorithm, or its variants. The EM algorithm is an iterative algorithm that finds local maximum likelihood estimates of the model parameters  $\boldsymbol{\theta}$  when the data are incomplete or are treated as incomplete. In the context of Gaussian mixture model, the sample of  $N$  observations from (14) are the observed data. We define the component indicator variable  $\mathbf{Z}$  for the row clusters such that  $Z_{ig} = 1$  if observation  $i$  belongs to group  $g$  and 0 otherwise. In the clustering context, the group memberships are unknown and thus, the component indicator variable  $Z_{ig}$  are treated as the unobserved latent variable.

The EM algorithm alternates between the expectation (E-step) and maximization (M-step) steps. In the E-step, we compute the expected value of the complete data log-likelihood function using the current parameter values  $\boldsymbol{\theta}^{(t)}$ . In the M-step, the algorithm finds the estimate of  $\boldsymbol{\theta}$  that maximizes the expected value of the log-likelihood from the E-step. For a  $G$ -component GMM, the expected value of the complete data log-likelihood function is

$$\sum_{i=1}^N \sum_{g=1}^G \hat{z}_{ig} \left[ \log \pi_g - \frac{1}{2} \log |\boldsymbol{\Sigma}_g| - \frac{1}{2} \text{tr} \left[ \boldsymbol{\Sigma}_g^{-1} (\mathbf{x}_i - \boldsymbol{\mu}_g)(\mathbf{x}_i - \boldsymbol{\mu}_g)^\top \right] \right],$$

where expected values of the latent variable  $z_{is}$  are

$$\hat{z}_{ig} = P(Z_{ig} = 1 | \mathbf{x}_i, \boldsymbol{\theta}) = \frac{\pi_g f(\mathbf{x}_i | \boldsymbol{\mu}_g, \boldsymbol{\Sigma}_g)}{\sum_{h=1}^G \pi_h f(\mathbf{x}_i | \boldsymbol{\mu}_h, \boldsymbol{\Sigma}_h)}. \quad (15)$$

For the M-step, the updates for the  $\boldsymbol{\theta}$  are:

$$\hat{\pi}_g = \frac{1}{N} \sum_{i=1}^N \hat{z}_{ig}, \quad \hat{\boldsymbol{\mu}}_g = \frac{\sum_{i=1}^N \hat{z}_{ig} \mathbf{x}_i}{\sum_{i=1}^N \hat{z}_{ig}}. \quad (16)$$

The maximum likelihood estimate of unconstrained  $\boldsymbol{\Sigma}_g$  is given by:

$$\hat{\boldsymbol{\Sigma}}_g = \mathbf{S}_g = \frac{\sum_{i=1}^N \hat{z}_{ig} (\mathbf{x}_i - \boldsymbol{\mu}_g)(\mathbf{x}_i - \boldsymbol{\mu}_g)^\top}{\sum_{i=1}^N \hat{z}_{ig}}. \quad (17)$$

To estimate a block-diagonal  $\boldsymbol{\Sigma}_g$ , we input the  $\mathbf{S}_g$  to one of the three proposed column clustering estimators (e.g. greedy, hierarchical, numerical). Then we compute the estimate of the block covariance matrix for the  $g^{th}$  component with  $K$  blocks as:

$$\sum_{k=1}^K \mathbf{D}_{kg} \mathbf{S}_g \mathbf{D}_{kg}^\top. \quad (18)$$

For initialization, we use the K-means algorithm (Forgy, 1965) to provide initial assignment of the latent variables  $z_{ig}$ . We use Aiken's acceleration based criteria (Böhning et al., 1994) to determine convergence of the EM algorithm using a tolerance of  $10^{-4}$ . To obtain row clustering memberships, we take the argmax over the set  $\{\hat{z}_{i1}, \dots, \hat{z}_{iG}\}$  and the column groups are obtain by examining at the matrices  $\mathbf{D}_k$ .

### 3.1 Estimating the Number of Row Clusters

Here, we study the estimation of the number of clusters by the proposed model and it's accuracy of selecting the number of row clusters given data generated from a



GMM with  $G = 3$  components. We consider two scenarios where generate data from  $\mathcal{N}(\boldsymbol{\mu}_g, \boldsymbol{\Sigma}_g)$  where the covariance matrix has a block diagonal structure and a general structure (or non-block diagonal structure).

We choose similar parameter values to the simulation from (Tu and Subedi, 2022).

In the first scenario, we set

$$\boldsymbol{\mu}_1 = (-5, -4, -3, -2, -1, 0, 1, 2)^\top,$$

$$\boldsymbol{\mu}_2 = (0, 1, 2, 3, 4, 5, 6, 7)^\top,$$

$$\boldsymbol{\mu}_3 = (5, 6, 7, 8, 9, 10, 11, 12)^\top$$

and the covariance matrices are block diagonal. In particular we set  $\boldsymbol{\Sigma}_1 = \text{diag}(\boldsymbol{\Sigma}_{11}, \boldsymbol{\Sigma}_{12}, \boldsymbol{\Sigma}_{13})$  where

$$\boldsymbol{\Sigma}_{11} = \begin{bmatrix} 2.5 & 0.5 & 0.5 \\ 0.5 & 3.5 & 0.5 \\ 0.5 & 0.5 & 4.5 \end{bmatrix}, \quad \boldsymbol{\Sigma}_{12} = \begin{bmatrix} 2 & 1 & 1 \\ 1 & 2 & 1 \\ 1 & 1 & 2 \end{bmatrix}, \quad \boldsymbol{\Sigma}_{13} = \begin{bmatrix} 3.5 & 3.0 \\ 3.0 & 3.9 \end{bmatrix},$$

and set  $\boldsymbol{\Sigma}_2 = \text{diag}(\boldsymbol{\Sigma}_{21}, \boldsymbol{\Sigma}_{22}, \boldsymbol{\Sigma}_{23})$  where

$$\boldsymbol{\Sigma}_{21} = \begin{bmatrix} 4.5 & -2 & 1 \\ -2 & 4.5 & 2 \\ 1 & 2 & 4.5 \end{bmatrix}, \quad \boldsymbol{\Sigma}_{23} = \begin{bmatrix} 4 & 2 \\ 2 & 4 \end{bmatrix}, \quad \boldsymbol{\Sigma}_{22} = \begin{bmatrix} 4 & 3 & 3 \\ 3 & 3.5 & 3 \\ 3 & 3 & 4 \end{bmatrix},$$

and set  $\Sigma_3 = \text{diag}(\Sigma_{31}, \Sigma_{32})$  where

$$\Sigma_{31} = \begin{bmatrix} 2.1 & 2 & 2 & 2 & 2 \\ 2 & 2.5 & 2 & 2 & 2 \\ 2 & 2 & 3 & 2 & 2 \\ 2 & 2 & 2 & 5 & 2 \\ 2 & 2 & 2 & 2 & 4 \end{bmatrix}, \quad \Sigma_{32} = \begin{bmatrix} 2 & 1 & 1 \\ 1 & 3.5 & 1 \\ 1 & 1 & 2.5 \end{bmatrix}.$$

In the second scenario, we set  $\Sigma_g$  to be different random positive-definite matrices generated by setting  $\Sigma_g = \mathbf{A}_g^T \mathbf{A}_g$  where the elements of  $\mathbf{A}_g$  are generated independently from the uniform distribution on the interval  $(0.0, 1.0)$ . This comparison considers what happens when the data is generated from a model that violates the bi-clustering framework or assumption of block-diagonal covariance matrix.

In both scenarios, we set  $\pi_1 = \pi_2 = \pi_3 = 1/3$  and we vary the number of observations per component. Then we chose the number of row cluster by iterating over the search space  $\hat{G} \in \{1 \dots 5\}$  and applying the BIC (Stoica and Selen, 2004; Schwarz, 1978) criterion to select the number of components. For both scenarios we replicate the experiment 100 times. We compare performance of the proposed method to the performance of a GMM.

Figure 7 shows the average estimated number of components with band showing plus/minus the standard deviation for bi-clustering and GMM under the two scenarios. Both panels show that the models select the true number of row clusters more often as the size of input data grows. However, in the left panel the bi-clustering model arrives to 100% accuracy earlier. On the other hand, the right panel shows

that a general covariance structure causes issues for the bi-clustering model which needs lots variable groups to achieve a good fit of the data. This provides some evidence that in the presence of a block-diagonal covariance matrix, the bi-clustering is efficient in determining the number of row clusters. In addition, Figure 13 in B summarizes the accuracy of identifying the correct number of groups.

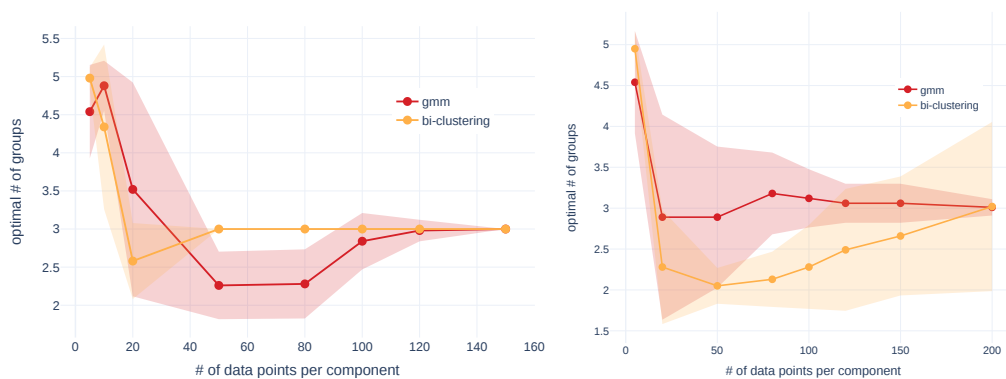


Figure 7: Recovery of the number of groups when the covariance structure is block diagonal (*Left*) and a random positive definite matrix (*Right*). Both panels display the average and plus/minus the standard deviation for a GMM and the proposed bi-clustering model when  $G = 3$  while varying the number of observations within each component.

### 3.2 Bi-Clustering Applications

In this subsection, we demonstrate the applicability of the proposed biclustering algorithms on benchmark datasets as well as high dimensional datasets from bioinformatics and topics modelling. We examine the row clustering performance of the proposed bi-clustering approach i.e., the Gaussian mixture model with a block-diagonal covariance matrix estimated by the hierarchical method. We compare the results of the proposed approach with  $K$ -means (Forgy, 1965), the unrestricted Gaussian

mixture model (Reynolds, 2009), and two other bi-clustering methods (UCUU by Tu and Subedi (2022) and spectral co-clustering Dhillon (2001)). We use  $K$ -means, GMM and spectral co-clustering implementations with their default parameters from the `sklearn` library (Pedregosa et al., 2011). Additionally, we implemented the factor-analyzer UCUU model by Tu and Subedi (2022) in Python.

### 3.2.1 Bi-clustering benchmark datasets

Here, we applied the algorithms on well-known low-dimensional benchmark datasets: **Wine** (Cortez et al., 2009), **Olive** (Forina and Tiscornia, 1982) and **Ecoli** (Nakai and Kanehisa, 1991). We scale the data to have the mean equal to 0 and variance equal to 1 prior to clustering. We compare the clustering performance using the adjusted rand index (ARI) (Rand, 1971; Hubert and Arabie, 1985; Zhang et al., 2012), accuracy and computational time. The results are summarized in Table 2.

Table 2: Average adjusted rand index (ARI), accuracy and execution time over 10 different runs of all algorithms on the given datasets.

Datasets	Wine			Olive			Ecoli		
	ARI	%, acc	time (in sec)	ARI	%, acc	time (in sec)	ARI	%, acc	time (in sec)
K-means	0.897	96.6%	0.015	0.448	76.5%	0.047	0.509	65.2%	0.036
GMM	0.831	92.7%	<b>0.009</b>	<b>0.601</b>	78.1%	<b>0.019</b>	0.646	74.4%	<b>0.015</b>
UCUU Model	<b>0.948</b>	<b>98.3%</b>	4.320	0.517	79.1%	19.62	—	—	—
Proposed	0.945	98.3%	0.120	0.574	<b>80.4%</b>	0.169	<b>0.656</b>	<b>76.2%</b>	0.138
Spectral co-clustering	0.738	90.9%	0.020	0.237	57.3%	0.042	0.394	56.4%	0.048

The proposed algorithm has similar accuracy compared to known row clustering algorithms and other bi-clustering approaches and even outperforms others on the **Ecoli** dataset. However, is almost  $10\times$  slower in terms of execution time than other listed approaches except for the UCUU model. The UCUU model, which is most

similar algorithm to our proposed method, runs  $400\times$  slower than  $K$ -means, GMM and spectral co-clustering. Thus, the proposed approach has an advantage in terms of lower execution time compared to the bi-clustering UCUU model, which is very similar in utility.

### 3.2.2 Bi-clustering in Bioinformatics

Biclustering is used in bioinformatics to simultaneously cluster observations and genes. Identifying groups of highly correlated genes that have different correlation structure in different groups of individuals (i.e., disease vs healthy individuals or between individuals with subtypes of diseases) can shed light into underlying biological mechanisms of disease development.

Here, we compare the algorithms' performance on the high-dimensional genomics classification problems using two benchmark gene expression datasets **Alon** (Alon et al., 1999) and **Golub** (Golub et al., 1999) available in the R package **plsgenomics** (Boulesteix et al., 2018). We applied our approach on two versions of the datasets: (i) a subset of 100 genes selected using ANOVA F-test (Feir-Walsh and Toothaker, 1974) which from here on is referred to as **Alon**<sub>100</sub> and (ii) full datasets where all available genes are used. The ANOVA F-test selects the set of  $K = 100$  features with highest ratio of explained to unexplained variance between the given ground truth groups. We applied our approach other competing approaches. Unfortunately, we were unable to run the UCUU model by Tu and Subedi (2022) on the full set of features because of (i) increasing computational time; (ii) authors' note that this algorithm is not designed for the scenario when the number of features is significantly higher than

the number of observations. Therefore, UCUU model was only applied to  $\text{Alon}_{100}$ .

The performance of the proposed algorithm along with comparisons with other approaches in terms of ARI and % accuracy on  $\text{Alon}_{100}$  and  $\text{Alon}_{\text{full}}$  datasets are provided in Table 3.

Table 3: ARI and accuracy of different algorithms on given high-dimensional datasets and their preprocessed versions with 100/150 features selected with ANOVA F-testFeir-Walsh and Toothaker (1974).

Datasets	$\text{Alon}_{100}$		$\text{Golub}_{150}$		$\text{Alon}_{\text{full}}$		$\text{Golub}_{\text{full}}$	
	ARI	%, acc	ARI	%, acc	ARI	%, acc	ARI	%, acc
K-means	0.510	86.0%	0.892	97.3%	-0.002	55.3%	0.162	70.8%
GMM	0.545	87.0%	<b>0.935</b>	<b>98.4%</b>	0.001	56.4%	0.161	53.2%
UCUU Model	<b>0.609</b>	<b>89.2%</b>	0.892	97.3%	—	—	—	—
Proposed	0.541	87.0%	0.892	97.3%	-0.006	54.8%	<b>0.212</b>	<b>73.6%</b>
Spectral co-clustering	0.541	87.0%	0.892	97.3%	<b>0.040</b>	<b>62.9%</b>	0.185	72.2%

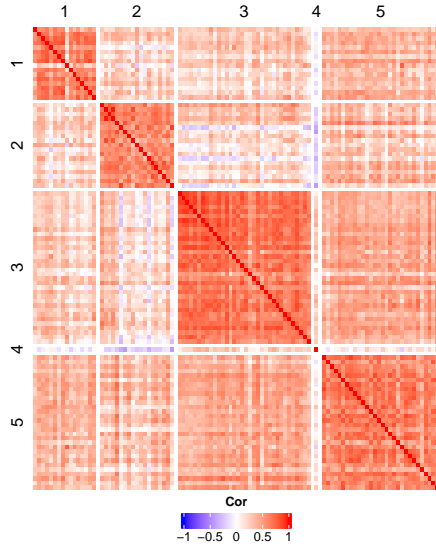
In the case of  $\text{Alon}_{100}$ , the UCUU model had a slightly higher ARI compared to the proposed model. However, our proposed method takes substantially less time to fit. Unfortunately, the performance of all methods degraded significantly on the full  $\text{Alon}$  dataset, with the Spector co-clustering method achieving maximum accuracy of 62.9%.

In Figure 8, we visualize the true and estimated correlation structures in the two estimated clusters of the  $\text{Alon}_{100}$  dataset. Note that column permutations are done to achieve a checkerboard-like structure as illustrated. As can be seen in Figure 8, the estimated column clusters are grouping variables that have high correlation (either positive or negative). This can provide valuable biological insight. For example, the variables X53586 (mRNA for integrin alpha 6), X54942 (ckshs2 - mRNA for Cks1 protein homologue) and X54941 (ckshs1 - mRNA for Cks1 protein homologue) are all assigned to column cluster 5 in Group 1 (with majority of tumour samples) indicating

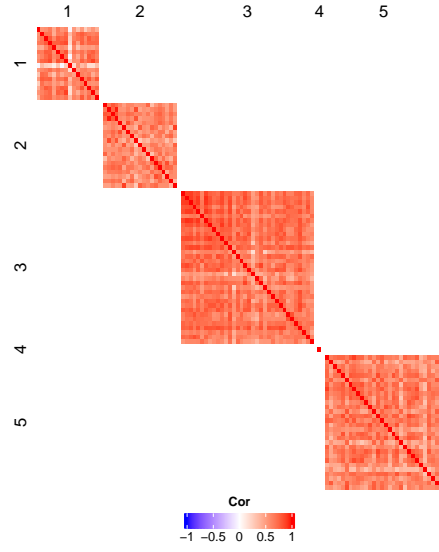
that they have a high correlation in tumour samples. Both integrin alpha 6 (Beaulieu, 2020) and Cks1 protein (Shapira et al., 2005) have previously been identified to play roles in colorectal cancer. On the other hand, in Group 2 (with majority of healthy samples), these variables were assigned to different column clusters: **X53586** was assigned to column cluster 1, **X54942** was assigned to column cluster 5 and **X54941** was assigned to column cluster 3, indicating that these variables have little to no correlation in healthy samples.

**Golub** dataset (Golub et al., 1999) comprises 2030 gene expressions of 72 patients, 47 of them are diagnosed with acute lymphoblastic leukemia (ALL) and 25 with acute myeloid leukemia (AML). Similar to the **Alon** dataset, we construct **Golub**<sub>150</sub> with subset of 150 features selected with ANOVA F-test (Feir-Walsh and Toothaker, 1974). We compare the performance of the proposed approach with competing approach on both the **Golub**<sub>150</sub> and the full dataset. Here, for the **Golub**<sub>150</sub> dataset, the GMM has the largest ARI slightly higher compared to our proposed model. However, due to the block diagonal covariance structure, our proposed method is more parsimonious than GMM. Moreover, the column clusters can provide valuable insights as illustrated below which the GMM lacks. Similar to the full **Alon** data, the performance of all methods degraded significantly on the full **Golub** dataset - in this case substantially for the GMM, while our proposed method achieves maximum accuracy of 73.6% among the competing models.

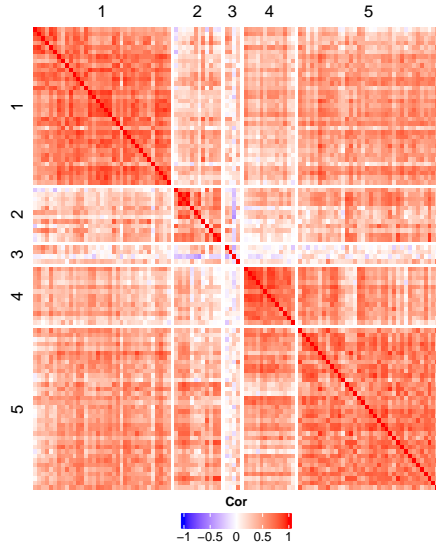
In Figure 9, we visualize the observed and estimated correlation structures in the two predicted clusters of the **Golub**<sub>150</sub> dataset. Column cluster 3 in Group 1 (i.e., the group comprising of all ALL samples) consists of 27 variables which have high



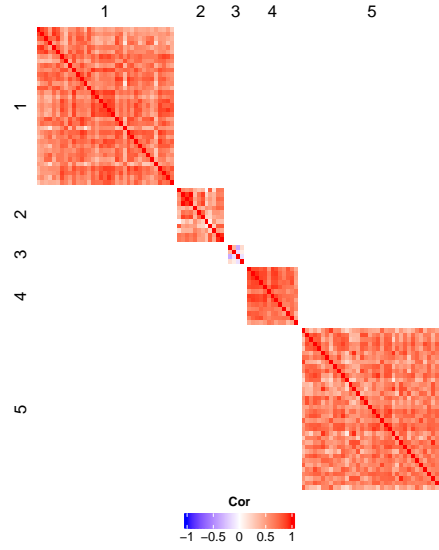
(a) Observed correlation of predicted Group 1



(b) Estimated correlation of predicted Group 1



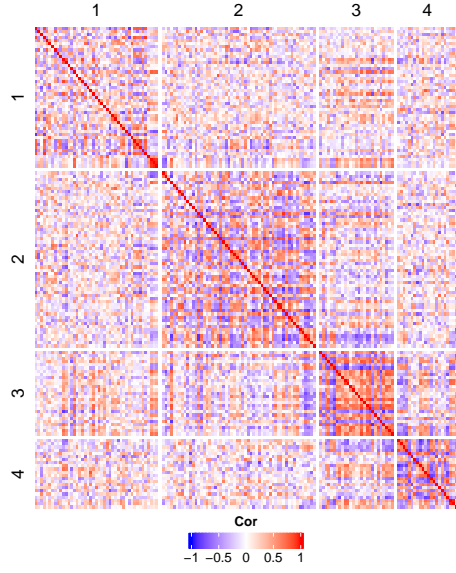
(c) Observed correlation of predicted Group 2



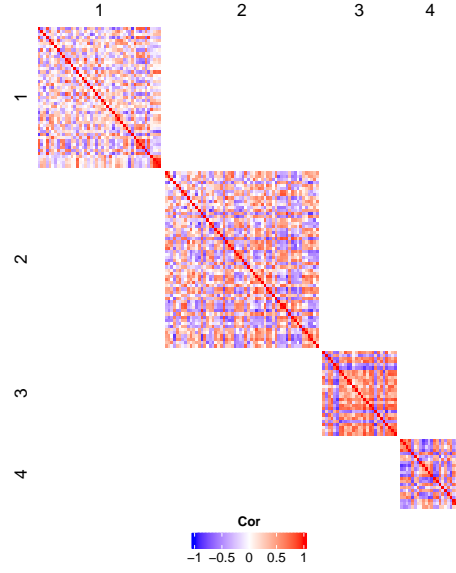
(d) Estimated correlation of predicted Group 2

Figure 8: True and estimated correlation matrices of the predicted groups from the  $\text{Alon}_{100}$  dataset. Note that most tumour samples were classified as Group 1 and most healthy samples were classified as Group 2.





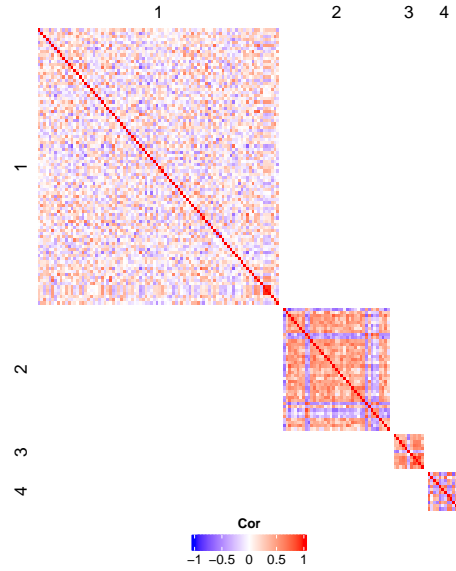
(a) Observed correlation of predicted Group 1



(b) Estimated correlation of predicted Group 1



(c) Observed correlation of predicted Group 2



(d) Estimated correlation of predicted Group 2

Figure 9: True and estimated correlation matrices of the predicted groups from the  $\text{Golub}_{150}$  dataset. Note that all 11 ALL samples were classified as Group 1 and 26 out of 27 AML samples were classified as Group 2.

correlations (either positive or negative) in the ALL samples. Out of the 27 variables, 24 of them were assigned to column cluster 1 in Group 2 (the group comprising of mostly AML samples). As evident from Figure 9, the magnitude of the correlations among the variables in column cluster 1 of Group 2 is lower compared to that of column cluster 3 of Group 1. Interestingly, pathway analysis using Reactome (Gillespie et al., 2022) identifies that 9 out of the above 24 genes are known to be involved in pathways related to platelet activation, signaling and aggregation. Platelets are specialized blood cells which are primarily responsible for preventing bleeding but are also recently found to promote tumor growth and metastasis (Yan and Jurasz, 2016). Furthermore, cancer cells have been shown to induce platelet activation and aggregation in several cancers, a phenomenon known as tumor cell-induced platelet aggregation (Jurasz et al., 2004). Investigating the differences in correlation structures among these genes between AML and ALL samples could provide valuable biological insight.

### 3.2.3 Bi-clustering in Topic Modelling

Topic Modelling Wallach (2006) is an area of Natural Language Processing that tries to find abstract human-interpretable topics in a collection of an arbitrary number of documents. Essentially, the problem of grouping documents into unsupervised topics can be solved by leveraging clustering techniques. Human language is incredibly complex. There are multiple possible groupings one can find in a set of documents, some having a stronger signals-no-noise ratio than others. e.g., Trip advisor’s hotel reviews can be grouped by review sentiment (recommend/do not recommend), hotel

geographical location or more generalized hotel features (has access to the beach, superb breakfast, polite managers etc.). Each of the clustering can be desired depending on the application. However, classical clustering algorithms will require additional data post-processing to provide interpretations of the topics they produce Sievert and Shirley (2014).

In this subsection, we apply the proposed bi-clustering algorithm to the topic modelling problem. We test our algorithm on two real-world datasets of customer reviews available on Kaggle. The first is Trip Advisor hotel Alam et al. (2016) data that consists of 20491 unique free-text hotel reviews accompanied by a numerical rating (from 1 to 5). The second one includes reviews and ratings of three Disneyland (Chillar, 2022) branches. We use only a subset of the data that reviews Disneyland Paris (13630 free-text responses). The language of reviews in both datasets is English. There are no reference labels available in this application. We aim to demonstrate that the proposed algorithm as a tool for summarizing customer reviews data.

For better explainability of the resulted topics and column groupings, we decided to apply the bi-clustering algorithm to the document-terms matrix instead of document-embeddings Grootendorst (2022) data type. Testing the proposed algorithm with semantic text embeddings is left for future work.

The entries of the document-terms matrix are term frequency-inverse document frequency scores (TF-IDF) Aizawa (2003). Let us define  $\text{tf}(t, d)$  as a relative frequency of the term  $t$  in some document  $d$ . Then, the inverse document frequency of the term  $t$  given a collection  $D$  of  $N$  documents is computed as  $\text{idf}(t, D) = \log \frac{N}{|d \in D: t \in d|}$ .

To simplify, the term frequency measures how frequent a term is for a given document. The inverse document frequency measures how rare this term is in the overall collection of documents. We define a TF-IDF score of a term  $t$  in the document  $d$  as  $\text{tf-idf}(t, d) = \text{tf}(t, d)\text{idf}(t, D)$ . The score is maximized when a specific term is frequent in a given document but uncommon for other documents. The TF-IDF score of the stop words is close to zero, as, by definition, stop words have a high probability of being present in every document in the collection.

Large collections of documents may include over a thousand unique words. Therefore, before fitting the bi-clustering model, we select only 1000 features with the highest average  $TF$  scores. Additionally, we utilize `SelectKBest` from the sklearn Pedregosa et al. (2011) Python library to select 400 terms that are the most predictive of the review rating.

Figure 10 and 11 demonstrate the column and row groupings for the Trip Advisor and Disneyland Paris data. The heatmap entries are computed as the average TF-IDF score of terms inside the column grouping  $A$  row cluster  $B$  divided by average TF-IDF scores of  $A$  among all row clusters and multiplied by 100%. This can be interpreted as how much "more important" a column cluster  $A$  is for a row cluster  $B$  than average.

From Figure 10, we infer that lower hotel ratings may be attributed to the cigarette smell, rude managers, dirty conditions, problems with the check desk and unexpected credit card charges. The highest ratings are correlated with access to public transport or the hotel's location within walking distance of the city's landmarks, friendly hotel staff and beautiful decorations of the premises. Figure 11

demonstrates that both feature clusters of food (ice cream and chips-burgers-fries) are highly associated with the lowest ratings of Disneyland Paris. It may signal that the food quality is lower than expected. At the same time, people are unhappy with closed attractions, rude staff, pushing and perhaps the fact that most people in Paris speak exclusively French.

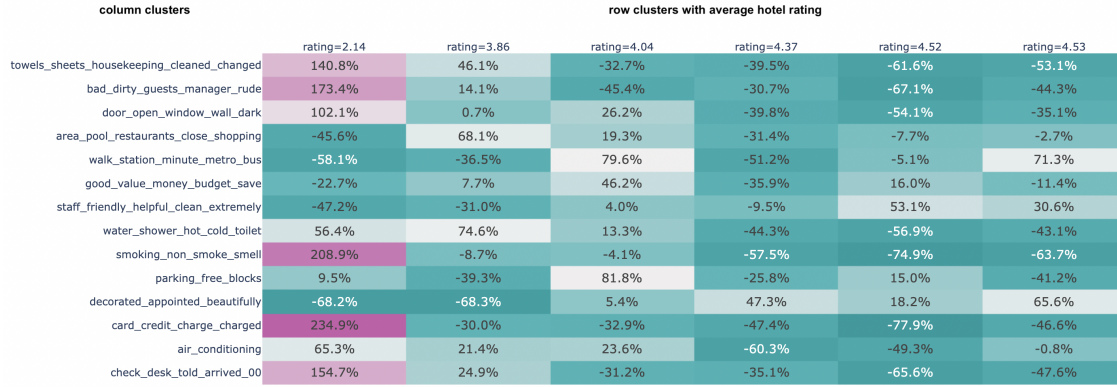


Figure 10: Resulting column and row clusters from the Trip Advisor hotel reviews. Entries of the heatmap represent how much “more important” a given column cluster is for a given row cluster than average.

## 4 Conclusions

In this work, we have proposed a bi-clustering algorithm based on a finite mixture of multivariate Gaussian models with block diagonal covariance structure. We demonstrated that our approach has a comparable clustering performance to the state-of-the-art algorithms in the field while providing substantial improvement in the computational time. We also illustrate the applicability of the proposed approach on real world datasets from various fields.

column clusters	row clusters with average rating			
	rating=3.23	rating=3.5	rating=4.13	rating=4.54
disney_park_amazing_paris_time	27.5%	7.2%	-12.9%	-21.7%
mountain_ride_space_buzz_laser	38.9%	-1.9%	-16.0%	-20.9%
rides_closed_attractions_attraction_technical	20.8%	-0.7%	-5.9%	-14.2%
years_ago_20_changed	64.2%	-18.4%	-22.7%	-23.0%
food_expensive_quality_poor_outlets	41.0%	-10.4%	-14.3%	-16.3%
chips_burger_fries_basic_burgers	173.8%	-49.0%	-62.6%	-62.3%
people_french_rude_way_pushing	35.3%	45.8%	-25.4%	-55.6%
cast_members	-50.7%	154.4%	-38.6%	-65.0%
looking_forward	63.7%	-0.9%	-16.8%	-46.0%
castle_beauty_sleeping	-21.9%	16.7%	13.4%	-8.3%
recommend_highly_recommended	-14.7%	-27.1%	21.8%	20.0%
ice_cream	134.7%	-12.7%	-48.5%	-73.5%
smoking_areas_smoke_designated_smokers	-8.7%	94.3%	-25.2%	-60.4%
staff_friendly_clean_helpful	-13.3%	32.4%	-10.3%	-8.7%
service_customer_slow	39.1%	57.2%	-36.8%	-59.5%

Figure 11: Resulting column and row clusters from the Disneyland Paris reviews. Entries of the heatmap represent how much “more important” a given column cluster is for a given row cluster than average.

## References

- Aizawa, A. (2003), ‘An information-theoretic perspective of tf-idf measures’, *Information Processing & Management* **39**(1), 45–65.
- Alam, M. H., Ryu, W.-J. and Lee, S. (2016), ‘Joint multi-grain topic sentiment: modeling semantic aspects for online reviews’, *Information Sciences* (339), 206–223.
- Alon, U., Barkai, N., Notterman, D., Gish, K., Ybarra, S., Mack, D. and Levine, A. (1999), ‘Alon u, barkai n, notterman da, gish k, ybarra s, mack d, levine ajbroad patterns of gene expression revealed by clustering analysis of tumor and normal colon tissues probed by oligonucleotide arrays. proc natl acad sci usa 96: 6745-

- 6750', *Proceedings of the National Academy of Sciences of the United States of America* **96**, 6745–50.
- Balcan, M.-F., Liang, Y. and Gupta, P. (2014), 'Robust hierarchical clustering', *The Journal of Machine Learning Research* **15**(1), 3831–3871.
- Beaulieu, J.-F. (2020), 'Integrin  $\alpha 6 \beta 4$  in colorectal cancer: expression, regulation, functional alterations and use as a biomarker', *Cancers* **12**(1), 41.
- Beeferman, D. and Berger, A. (2000), Agglomerative clustering of a search engine query log, in 'Proceedings of the sixth ACM SIGKDD international conference on Knowledge discovery and data mining', pp. 407–416.
- Ben-Dor, A., Chor, B., Karp, R. and Yakhini, Z. (2002), Discovering local structure in gene expression data: the order-preserving submatrix problem, in 'Proceedings of the sixth annual international conference on Computational biology', pp. 49–57.
- Bergmann, S., Ihmels, J. and Barkai, N. (2003), 'Iterative signature algorithm for the analysis of large-scale gene expression data', *Physical review E* **67**(3), 031902.
- Berkhin, P. (2006), A survey of clustering data mining techniques, in 'Grouping multidimensional data', Springer, pp. 25–71.
- Bhatia, P., Iovleff, S. and Govaert, G. (2014), 'blockcluster: An r package for model based co-clustering', *Journal of Statistical Software* **76**.
- Böhning, D., Dietz, E., Schaub, R., Schlattmann, P. and Lindsay, B. (1994), 'The distribution of the likelihood ratio for mixtures of densities from the one-parameter exponential family', *Annals of the Institute of Statistical Mathematics* **46**, 373–388.

- Boulesteix, A.-L., Durif, G., Lambert-Lacroix, S., Peyre, J. and Strimmer., K. (2018), *plsgenomics: PLS Analyses for Genomics*. R package version 1.5-2.  
**URL:** <https://CRAN.R-project.org/package=plsgenomics>
- Broto, B., Bachoc, F., Clouvel, L. and Martinez, J.-M. (2022), ‘Block-diagonal covariance estimation and application to the shapley effects in sensitivity analysis’, *SIAM/ASA Journal on Uncertainty Quantification* **10**(1), 379–403.
- Busygin, S., Prokopyev, O. and Pardalos, P. M. (2008), ‘Biclustering in data mining’, *Computers & Operations Research* **35**(9), 2964–2987.
- Cheng, Y. and Church, G. M. (2000), Biclustering of expression data, *in* ‘Proc Int Conf Intell Syst Mol Biol.’, Vol. 8, pp. 93–103.
- Chillar, A. (2022), ‘Tripadvisor disneyland reviews dataset’.  
**URL:** <https://www.kaggle.com/datasets/arushchillar/disneyland-reviews>
- Cortez, P., Cerdeira, A., Almeida, F., Matos, T. and Reis, J. (2009), ‘Modeling wine preferences by data mining from physicochemical properties’, *Decision support systems* **47**(4), 547–553.
- Dempster, A. P., Laird, N. M. and Rubin, D. B. (1977), ‘Maximum likelihood from incomplete data via the em algorithm’, *Journal of the Royal Statistical Society: Series B (Methodological)* **39**(1), 1–22.
- Dhillon, I. S. (2001), Co-clustering documents and words using bipartite spectral graph partitioning, *in* ‘Proceedings of the seventh ACM SIGKDD international



- conference on Knowledge discovery and data mining', KDD '01, Association for Computing Machinery, New York, NY, USA, pp. 269–274.
- Diday, E. and Simon, J. (1976), Clustering analysis, *in* 'Digital pattern recognition', Springer, pp. 47–94.
- Erica, E., Handari, B. and Hertono, G. (2018), Agglomerative clustering and genetic algorithm in portfolio optimization, *in* 'AIP Conference Proceedings', Vol. 2023, AIP Publishing LLC, p. 020217.
- Feir-Walsh, B. J. and Toothaker, L. E. (1974), 'An empirical comparison of the anova f-test, normal scores test and kruskal-wallis test under violation of assumptions', *Educational and Psychological Measurement* **34**(4), 789–799.
- Forgy, E. W. (1965), 'Cluster analysis of multivariate data: efficiency versus interpretability of classifications', *biometrics* **21**, 768–769.
- Forina, M. and Tiscornia, E. (1982), 'Pattern-recognition methods in the prediction of italian olive oil origin by their fatty-acid content', *Annali di Chimica* **72**(3-4), 143–155.
- Friedman, J., Hastie, T. and Tibshirani, R. (2008), 'Sparse inverse covariance estimation with the graphical lasso', *Biostatistics* **9**(3), 432–441.
- Gallaughher, M. P. B., Biernacki, C. and McNicholas, P. D. (2022), 'Parameter-wise co-clustering for high-dimensional data', *Computational Statistics* .

- Gillespie, M., Jassal, B., Stephan, R., Milacic, M., Rothfels, K., Senff-Ribeiro, A., Griss, J., Sevilla, C., Matthews, L., Gong, C. et al. (2022), ‘The reactome pathway knowledgebase 2022’, *Nucleic Acids Research* **50**(D1), D687–D692.
- Golub, T. R., Slonim, D. K., Tamayo, P., Huard, C., Gaasenbeek, M., Mesirov, J. P., Coller, H., Loh, M. L., Downing, J. R., Caligiuri, M. A., Bloomfield, C. D. and Lander, E. S. (1999), ‘Molecular classification of cancer: Class discovery and class prediction by gene expression monitoring’, *Science* **286**(5439), 531–537.
- Grootendorst, M. (2022), ‘Bertopic: Neural topic modeling with a class-based tf-idf procedure’.
- Gu, J. and Liu, J. S. (2008), ‘Bayesian biclustering of gene expression data’, *BMC genomics* **9**(1), 1–10.
- Hartigan, J. A. (1972), ‘Direct clustering of a data matrix’, *Journal of the american statistical association* **67**(337), 123–129.
- Hemmecke, R., Köppe, M., Lee, J. and Weismantel, R. (2009), Nonlinear integer programming, in ‘50 Years of Integer Programming 1958-2008’, Springer Berlin Heidelberg, pp. 561–618.
- Hubert, L. and Arabie, P. (1985), ‘Comparing partitions’, *Journal of Classification* **2**, 193–218.
- Jurasz, P., Alonso-Escolano, D. and Radomski, M. W. (2004), ‘Platelet–cancer interactions: mechanisms and pharmacology of tumour cell-induced platelet aggregation’, *British journal of pharmacology* **143**(7), 819.

- Khan, K., Rehman, S. U., Aziz, K., Fong, S. and Sarasvady, S. (2014), Dbscan: Past, present and future, *in* ‘The fifth international conference on the applications of digital information and web technologies (ICADIWT 2014)’, IEEE, pp. 232–238.
- Kluger, Y., Basri, R., Chang, J. and Gerstein, M. (2003), ‘Spectral biclustering of microarray data: Coclustering genes and conditions’, *Genome research* **13**, 703–16.
- Ledoit, O. and Wolf, M. (2004), ‘A well-conditioned estimator for large-dimensional covariance matrices’, *Journal of Multivariate Analysis* **88**(2), 365–411.
- Madeira, S. C. and Oliveira, A. L. (2004), ‘Biclustering algorithms for biological data analysis: a survey’, *IEEE/ACM transactions on computational biology and bioinformatics* **1**(1), 24–45.
- Madeira, S. C., Teixeira, M. C., Sa-Correia, I. and Oliveira, A. L. (2008), ‘Identification of regulatory modules in time series gene expression data using a linear time biclustering algorithm’, *IEEE/ACM Transactions on Computational Biology and Bioinformatics* **7**(1), 153–165.
- Martella, F., Alfò, M. and Vichi, M. (2008), ‘Biclustering of gene expression data by an extension of mixtures of factor analyzers’, *The International Journal of Biostatistics* **4**.
- McInnes, L., Healy, J. and Astels, S. (2017), ‘hdbscan: Hierarchical density based clustering.’, *J. Open Source Softw.* **2**(11), 205.
- McNicholas, P. D. and Murphy, T. B. (2008), ‘Parsimonious gaussian mixture models’, *Statistics and Computing* **18**, 285–296.

- Milligan, G. W. and Cooper, M. C. (1987), ‘Methodology review: Clustering methods’, *Applied psychological measurement* **11**(4), 329–354.
- Murtagh, F. and Legendre, P. (2014), ‘Ward’s hierarchical agglomerative clustering method: which algorithms implement ward’s criterion?’, *Journal of classification* **31**(3), 274–295.
- Nakai, K. and Kanehisa, M. (1991), ‘Uci machine learning repository’, *URL: <https://archive.ics.uci.edu/ml/datasets/ecoli>*.
- Padilha, V. A. and Campello, R. J. (2017), ‘A systematic comparative evaluation of biclustering techniques’, *BMC bioinformatics* **18**(1), 1–25.
- Pedregosa, F., Varoquaux, G., Gramfort, A., Michel, V., Thirion, B., Grisel, O., Blondel, M., Prettenhofer, P., Weiss, R., Dubourg, V., Vanderplas, J., Passos, A., Cournapeau, D., Brucher, M., Perrot, M. and Duchesnay, E. (2011), ‘Scikit-learn: Machine learning in Python’, *Journal of Machine Learning Research* **12**, 2825–2830.
- Rand, W. M. (1971), ‘Objective criteria for the evaluation of clustering methods’, *Journal of the American Statistical Association* **66**(336), 846–850.
- Reynolds, D. A. (2009), ‘Gaussian mixture models.’, *Encyclopedia of biometrics* **741**(659-663).
- Rousseeuw, P. J. (1987), ‘Silhouettes: A graphical aid to the interpretation and validation of cluster analysis’, *Journal of Computational and Applied Mathematics* **20**, 53–65.

- Rugeles, D., Zhao, K., Gao, C., Dash, M. and Krishnaswamy, S. (2017), Biclustering: An application of dual topic models, *in* ‘Proceedings of the 2017 SIAM International Conference on Data Mining’, SIAM, pp. 453–461.
- Schwarz, G. (1978), ‘Estimating the dimension of a model’, *The Annals of Statistics* **6**(2), 461–464.
- Shapira, M., Ben-Izhak, O., Linn, S., Futerman, B., Minkov, I. and Hershko, D. D. (2005), ‘The prognostic impact of the ubiquitin ligase subunits skp2 and cks1 in colorectal carcinoma’, *Cancer* **103**(7), 1336–1346.
- Sievert, C. and Shirley, K. (2014), Ldavis: A method for visualizing and interpreting topics, *in* ‘Proceedings of the workshop on interactive language learning, visualization, and interfaces’, pp. 63–70.
- Sokal, R. R. and Michener, C. D. (1958), ‘A statistical method for evaluating systematic relationships’, *University of Kansas science bulletin* **38**, 1409–1438.
- Stoica, P. and Selen, Y. (2004), ‘Model-order selection: a review of information criterion rules’, *IEEE Signal Processing Magazine* **21**(4), 36–47.
- Tu, W. and Subedi, S. (2022), ‘A family of mixture models for biclustering’, *Statistical Analysis and Data Mining: The ASA Data Science Journal* **15**, 206 – 224.
- Vijaya, Sharma, S. and Batra, N. (2019), Comparative study of single linkage, complete linkage, and ward method of agglomerative clustering, *in* ‘2019 International Conference on Machine Learning, Big Data, Cloud and Parallel Computing (COMITCon)’, pp. 568–573.

- Wallach, H. M. (2006), Topic modeling: beyond bag-of-words, *in* ‘Proceedings of the 23rd international conference on Machine learning’, pp. 977–984.
- Wang, Y. K., Print, C. G. and Crampin, E. J. (2013), ‘Biclustering reveals breast cancer tumour subgroups with common clinical features and improves prediction of disease recurrence’, *BMC Genomics* **14**, 1–15.
- Wong, M., Mutch, D. and McNicholas, P. (2017), ‘Two-way learning with one-way supervision for gene expression data’, *BMC Bioinformatics* **18**.
- Yan, M. and Jurasz, P. (2016), ‘The role of platelets in the tumor microenvironment: from solid tumors to leukemia’, *Biochimica et Biophysica Acta (BBA)-Molecular Cell Research* **1863**(3), 392–400.
- Zhang, S., Wong, H.-S. and Shen, Y. (2012), ‘Generalized adjusted rand indices for cluster ensembles’, *Pattern Recognition* **45**(6), 2214–2226.

## A Standard Deviations for recovering the block-diagonal covariance matrix

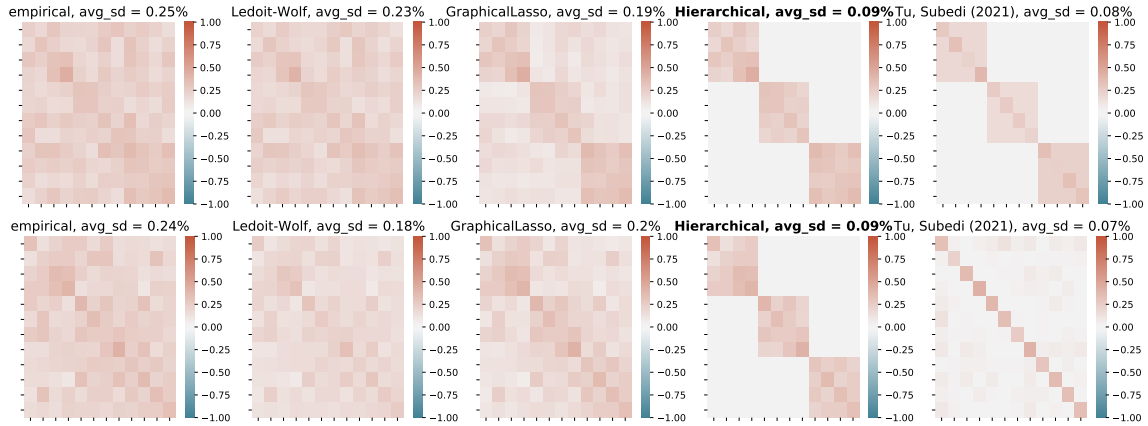


Figure 12: Standard deviations over ten runs of recovering block-diagonal covariance matrix with only positive (*top*) / negative (*bottom*) off-diagonal entries with five methods including MLE (empirical), Ledoit-Wolf, Graphical Lasso, Hierarchical (proposed) & UCUU method from Tu, Subedi 2021 Tu and Subedi (2022)

## B Accuracy for selecting the number of components

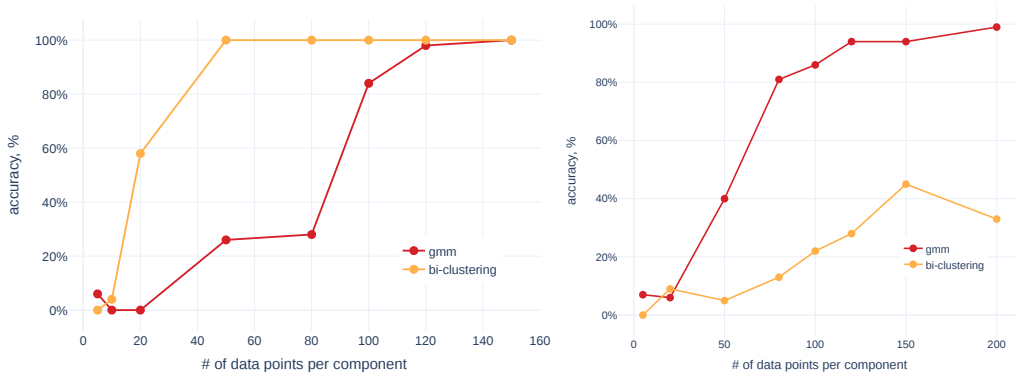


Figure 13: Accuracy of the number of groups when the covariance structure is block diagonal (*Left*) and a random positive definite matrix (*Right*) for the GMM and the proposed bi-clustering model when  $G = 3$  while varying the number of observations within each component.